This article is a post-print copy of M. Thunga, K. Chen, M. R. Kessler: Bio-renewable Precursor Fibers from Lignin/Polylactide Blends for Conversion to Carbon Fibers, *Carbon*, 2014, 68, 159-166 doi:10.1016/j.carbon.2013.10.075.

Bio-renewable precursor fibers from lignin/polylactide blends for conversion to carbon fibers

Mahendra Thunga[a, b], Keke Chen[a], David Grewell[c], Michael R. Kessler[a, b, d]

[a] Department of Materials Science and Engineering, Iowa State University, Ames, IA, USA
[b] Ames Laboratory, US Department of Energy, Ames, IA, USA
[c] Department of Agricultural and Biosystems Engineering, Iowa State University, Ames 50011, IA, USA
[d] School of Mechanical and Materials Engineering, Washington State University, Pullman, WA, USA

Abstract

Lignin, a highly aromatic biopolymer extracted as a coproduct of wood pulping, was investigated as a suitable precursor for carbon fibers. Lignin was chemically modified and blended with poly(lactic acid) (PLA) biopolymer before melt spinning into lignin fibers. The chemical modification of raw lignin involved butyration to form ester functional groups in place of polar hydroxyl (–OH) groups, which enhanced the miscibility of lignin with PLA. Fine fibers were extracted and spooled continuously from lignin/PLA blends with an overall lignin concentration of 75 wt.%. The influence of chemical modification and physical blending of lignin with PLA on the resulting fiber was studied by analyzing the microstructure of the fibers using transmission electron microscopy (TEM) and scanning electron microscopy (SEM). The influence of blend composition on the phase behavior was studied by differential scanning calorimetry (DSC). The effect of composition on the mechanical properties was studied by tensile tests of the lignin/PLA blend fibers. The thermal stability and carbon yield of the blended fibers with different concentrations of lignin were characterized by thermogravimetric analysis (TGA). The microstructure analysis of carbon fibers produced from lignin/PLA blends revealed composition dependent microporous structures inside the fine fibers.

1. Introduction

Carbon fiber based polymer composites have been recognized as advanced materials for structural applications. The unique reinforcing abilities of carbon fibers with their combination of high strength, low mass, and excellent fatigue resistance have made carbon fiber based composites exceptional compared to other fiber reinforced composites [1].However, the high cost of precursor materials for carbon fibers (which accounts for 51% of the cost of carbon fiber production) has limited the widespread applicability of carbon fibers [2], [3] and [4].

Lignin is an aromatic biopolymer and has been investigated as a precursor for the production of carbon fibers because of its low cost and bio-renewable nature [5]. The molecular structure of lignin consists of repeating units of the phenylpropane: *p*-coumaryl alcohol, coniferyl alcohol, and sinapyl alcohol [6], which makes it highly polar with a large number of hydroxyl (–OH)

groups. The production of carbon fiber from low-cost renewable resources such as lignin has been hindered by difficulties in processing fine lignin fibers. Its complex, interconnected structure makes it difficult to spin and spool raw lignin into fibers without modifications.

It is recognized that blending lignin with polymers is a convenient and inexpensive method to produce fibers with desired surface characteristics and mechanical properties. In previous studies, polyethylene terephthalate (PET), polypropylene (PP), and poly(ethylene oxide) (PEO) were successfully blended with lignin to produce fibers [7], [8] and [9]. However, developing a precursor utilizing a petroleum-based polymer may pose future problems considering limited oil reserves, which ultimately results in high price volatility for the precursor. A potential alternative to synthetic polymers is a biorenewable polymer acting as a plasticizer in the fiber spinning process. Polylactic acid (PLA) is a biopolymer derived from corn starch and sugarcane biomass [10] and [11]. Compared to traditional petroleum-based polymers used previously for plasticizing lignin, the crystallinity in bio-based PLA was observed to improve rheological properties of the melt. In addition, strain hardening, which favors processability of polymer melts, was observed in PLA when co-blended with an enantiomer [12]. Blending lignin with PLA not only offers the potential to make the carbon fiber production process greener and renewable, but also provides a low cost alternative precursor that allows for the processing of lignin fibers using conventional polymer processing techniques, such as melt spinning. However, the miscibility of lignin with a variety of plasticizing polymers is limited because of the presence of a large number of hydroxyl (–OH) groups. Adjusting the miscibility between lignin and PLA on the molecular level is essential to produce fine precursor fibers. Glasser et al. [13] and [14] have chemically modified lignin and found that esterification of lignin was more promising in enhancing its solubility in various organic solvents. The plasticization caused by esterification decreased the glass transition temperature (T_g) of lignin. Further, lignin was observed to be melt processable after esterification [15], [16] and [17]. Wool et al. [18] have studied the effect of esterification of lignin by butyration to improve the solubility of lignin in styrene, a reactive diluent commonly used in polyester resins. In the present work, efforts were made to modify lignin by esterification to enhance its molecular level miscibility with PLA.

Porous or activated carbon fibers are also widely used for water purification and gas separation applications [19]. The specific absorption properties of porous carbon fibers have made them the material of choice for advanced applications such as electrochemical super-capacitors, hydrogen storage, and catalyst support [20]. Over the past decade, novel precursors and processing techniques have been developed to produce porous carbon materials [20] and [21]. Most of these research efforts were primarily focused on either enhancing the micro-porous surface area or controlling the porosity in the fibers. Ji et al. [22] studied the effect of blending PLA biopolymer as a pore generating phase with polyacrylonitrile (PAN) as a conventional carbon forming precursor to produce porous carbon fibers. The pore size, surface area, and volume were strongly influenced by the PAN/PLA blend composition. However, most of the studies were based on solution spinning processing techniques which require solvent extraction.

In the present work, softwood kraft lignin was modified and blended with PLA biopolymer to show that chemically modified lignin is compatible with PLA. Blends of the modified lignin and PLA were successfully melt-spun into fine fibers. The physical interaction between the blend components responsible for the development of miscibility at the molecular level in the fine

fibers was investigated. The degree of phase compatibility was qualitatively studied by microscopic techniques and thermal analysis. The optimum blend composition necessary for producing continuous, fine fibers with high carbon yield after carbonization was investigated. Finally, the lignin-based precursor fibers were carbonized and the influence of PLA concentration on the porosity of the final carbon fibers was investigated systematically.

2. Experimental

2.1. Materials

Softwood kraft lignin (Indulin-AT) was provided by MeadWestvaco Corp., Richmond, VA. It was used as received and washed in dilute HCl solution (pH below 5) for 10 min to remove dissolved salts. The acid treated lignin was washed repeatedly with distilled water to neutralize the pH value. The washed lignin was vacuum-dried for several hours to remove the moisture content and then stored in dry air. Polylactide (PLA) was purchased from NatureWorks LLC, Minnetonka, MN. Butyric anhydride and 1-methylimidazole (1MIM) were purchased from Sigma–Aldrich and used as received. Deuterated dimethyl sulfoxide (DMSO-d6) used for NMR analysis was purchased from Cambridge Isotope Laboratories, Inc., Andover, MA. Potassium bromide (KBr) used for IR analysis was purchased from Fisher Scientific, Waltham, MA.

2.2. Blend preparation for fiber spinning

Lignin was butyrated prior to blending with PLA using the procedure described by Thielemans et al. [18]. Preparation and properties of butyrated lignin (B-lignin) is described in the supporting information. The degree of esterification of lignin was characterized. All the B-lignin/PLA blends were processed by melt mixing at 180 °C using a twin screw microcompounder from DACA Instruments, Santa Barbara, CA. The blends were processed by keeping the speed of the twin screws constant at 60 rpm. The residence time of the melt in the barrel was limited to 5 min to avoid thermal degradation. Fine fibers were extruded by a fiber spinning die attached to the end of the extruder. The extruded fiber was continuously spooled from the microcompounder with the help of an advanced DSM-Xplore micro fiber spinning device, DSM, Geleen, Netherlands. A constant stretching in the fibers was achieved by maintaining the speed of the winding drum constant.

2.3. Thermal and mechanical analysis

The influence of blend composition on the phase behavior was studied by differential scanning calorimetry (DSC). The glass transition (T_g) and melting (T_m) behavior of lignin/PLA blends was measured by DSC tests using a DSC-Q20 from TA Instruments. DSC scans were run from −50 to 200 °C at a heating rate of 20 °C/min under nitrogen atmosphere. The thermal stability and the carbon yield in all blend compositions were determined by thermogravimetric analysis (TGA) using a TGA-Q50 from TA Instruments. TGA results were obtained under nitrogen atmosphere from room temperature (RT) to 1000 °C at a heating rate of 20 °C/min. Tensile tests were performed using a dynamic mechanical analyzer (DMA) (Model Q800, TA Instruments) equipped with tensile clamps in iso-strain mode. The tests were conducted on fine fibers with

diameters ranging from 100 to 200 μm. Stress–strain curves were measured by stretching the fibers at a strain rate of 50 μm/min.

2.4. Characterization of morphology

The overall structure and the cross-section images of lignin/PLA fibers before and after carbonization were characterized using a FEI Quanta 250 Field Emission scanning electron microscope at 10.00 kV under vacuum. The morphology determined by transmission electron microscopy (TEM) on a 2007 JEOL 2100 200 kV scanning and transmission electron microscope (STEM) revealed the phase segregation of lignin and PLA in the blend fibers.

2.5. Heat treatment of fibers: stabilization and carbonization

The precursor fibers were converted into carbon fibers by thermal stabilization followed by carbonization using the heat treatment procedure developed by Lue [23] for preparing lignin based carbon fibers. The precursor fibers were placed in a porcelain crucible and heated to 105 °C at 1 °C/min to eliminate all moisture and then heated to 250 °C at a rate of 0.25 °C/min and held for 5 h in an oxygen stream to stabilize the fibers. The fibers were carbonized under nitrogen atmosphere at 1000 °C at a heating rate of 180 °C/h. Surface area and pore properties of the carbon fibers were characterized using a Micromeritics ASAP 2020 Surface Area and Porosity Analyzer (Micromeritics, Norcross, GA).

3. Results and discussion

3.1. Morphology of B-lignin/PLA blend fibers

Lignin chemically modified by butyration (B-lignin) was successfully melt-processed into fine fibers. Fig. 1a depicts melt processed B-lignin fiber spools and B-lignin/PLA blend fiber spools. As-received softwood lignin is difficult to process because of its molecular structure. Kubo et al. reported that melt processing of softwood kraft lignin was difficult even after blending with a plasticizing agent [8] and [24]. The presence of high guaiacyl monolignin units in the three-dimensional lignin macromolecule was recognized as the key factor effecting the processability of lignin. These repeating monolignin units with active hydroxyl (–OH) functional groups resulted in an increase in inter- and intra-molecular crosslinking. Replacing the hydroxyl groups (–OH) on lignin with ester groups (–O-alkyl) reduced the crosslinking ability of lignin and enhanced the melt processability [15]. Although the esterification reduces the concentration of hydroxyl groups (–OH) on lignin, some aliphatic –OH group are expected to be unaffected during the modification. These residual hydroxyl groups could promote crosslinking in the lignin/PLA fibers during the stabilization step. To facilitate fiber formation, all blends were processed at 180 °C, which is above the melting temperature of PLA. As a result of the aromatic molecular structure of lignin, fibers with 90 and 100 wt.% of lignin were brittle and difficult to handle during post processing at room temperature.

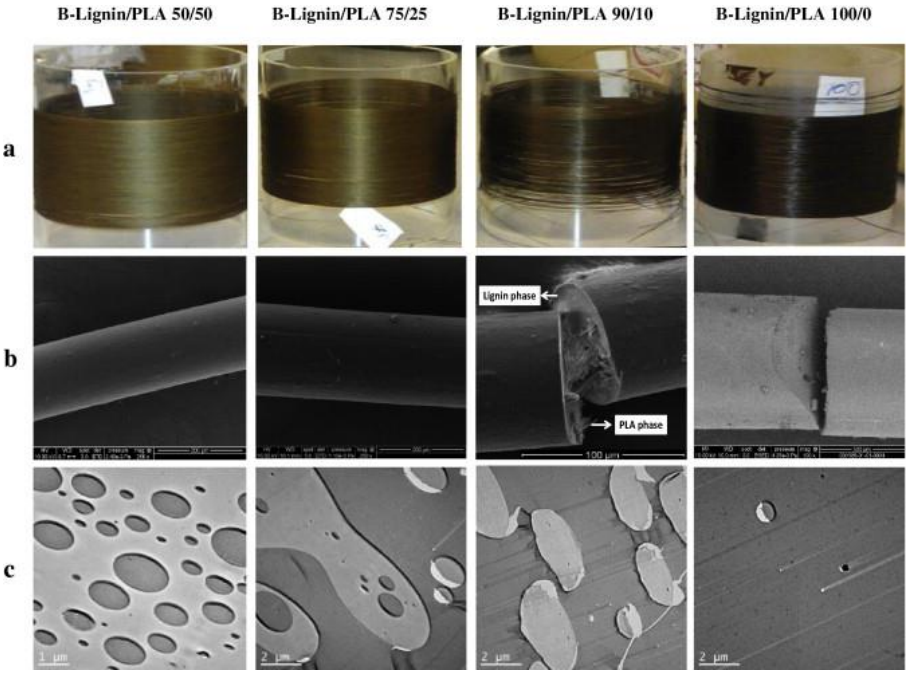

Fig. 1: Continuously spooled fibers of B-lignin/PLA blends (concentration of B-lignin increasing from left to right). (a) Fibers spooled on Pyrex glass mandrels. (b) SEM images of blend fibers showing overall structure of fibers. (c) Morphology of phase separation from cross section surface of individual blend fibers observed using TEM.

Esterification of lignin improved the processability of raw lignin and also enhanced the miscibility of lignin and PLA in the blends. The surface morphology of fibers extracted by melt spinning was initially examined by scanning electron microscopy (SEM) to determine the influence of phase compatibility on the structure of the fibers. Fig. 1b shows that all B-lignin/PLA blend fibers exhibited a uniform cylindrical structure independent of the composition of the blends. Macrophase separation, typically observed in immiscible blends, did not occur here. The cross-section SEM morphology of the fibers spun from B-lignin/PLA 75/25 blends with a diameter of ~200 μm showed that many small fibers are aligned inside the bulk fiber, resulting in micro-fiber reinforcement inside the larger fibers. The presence of such fine fibers inside the bulk fibers revealed that bi-component fibers were formed as a result of microphase separation between B-lignin and PLA in the blend fibers.

In order to further describe the phase behavior of the blends, the morphologies of the fiber cross-sections for the investigated blend compositions were examined by TEM, as shown in Fig. 1c. Although the overall structure of the bulk fibers appeared to be homogeneous and uniform, the TEM micrographs revealed microphase separation in all blends. The dark and bright regions in the TEM images correspond to the B-lignin and PLA phases, respectively. The difference in brightness of the phases is caused by the difference in electron densities between the two phases. The cross-section morphologies appeared to be strongly dependent on the composition of the blends. A systematic transition in phase separation was evident with the increase in B-lignin concentration in the blends. The morphologies changed from discontinuous B-lignin rich spherical phases (50 wt.% B-lignin) to co-continuous (75 wt.% B-lignin) back to discontinuous

PLA rich phases with increasing B-lignin concentration in the blends. The morphology of the discontinuous phases in 50 and 90 wt.% B-lignin blends was driven by phase segregation in the form of fine fibers aligned parallel to the fiber axes inside the bulk fiber. The phase separation of these bi-component fibers is schematically shown in Fig. 2 for 90 wt.% B-lignin blend fibers. Fine fibers with diameters on the nanometer scale extending from the cross-section surface can be clearly seen in the corresponding SEM image (Fig. 1b for 90/10 B-lignin/PLA blends). In contrast to the discontinuous phase separation in B-lignin/PLA 50/50 and 90/10 blends, the 75/25 blend showed B-lignin and PLA phases embedded in each other, which may result in stronger physical interaction between the two phases.

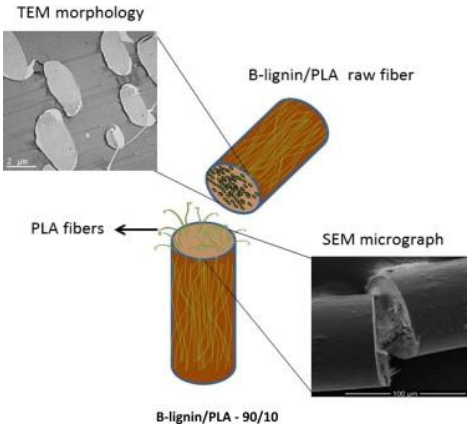

Fig. 2: Composite image showing the cross-section morphology and overall microstructure of B-lignin/PLA 90/10 blend fibers with PLA-rich phases self-assembled as micro fibers inside the bulk fiber.

3.2. Phase behavior of B-lignin/PLA blends

The interaction between the B-lignin and PLA phases in the blends was investigated based on their glass transition (T_g) and melting (T_m) behaviors. Fig. 3 show the DSC traces of investigated blend samples. The glass transition behavior of pure PLA showed a sharp transition compared to that of pure B-lignin, which extended over a broad temperature range. It is important to note, the T_g's of the PLA and B-lignin phases overlapped each other. The broad T_g observed for B-lignin was caused by the complex molecular structure that resulted in multiple relaxation phases within the same transition temperature range. With the increase in B-lignin concentration in the blends, the onset of T_g shifted to lower temperatures and the transition became broader. Table 1 shows the T_g's for all blends as determined from the DSC curves. The T_g of pure PLA decreased from 60 to 53 °C with the incorporation of 50 wt.% of B-lignin in the blend. On further increase in B-lignin concentration, the T_g reduced to 44 °C for the B-lignin/PLA 90/10 blend. The shift in T_g with change in blend composition was attributed to molecular level interactions between the blend components. Lignin may act as a nucleation sight producing smaller spherulites resulting in reduction of the amorphous phase. In addition to that, lignin may freeze the amorphous phase faster resulting in more free volume to reduce the T_g.

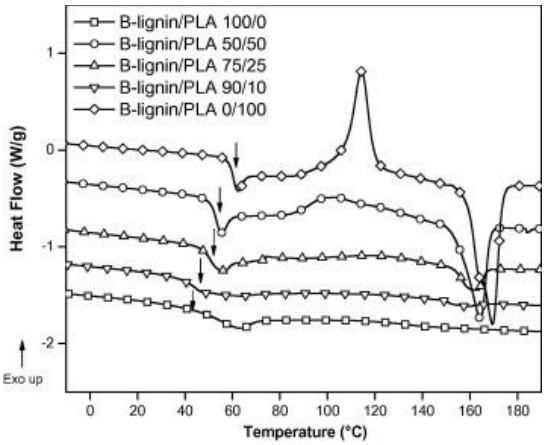

Fig. 3: Differential scanning calorimetry (DSC) curves for B-lignin/PLA blends.

Table 1: Glass transition temperature (T_g), melting temperature (T_m), and enthalpy of crystallization for B-lignin/PLA blends.

Sample	T_g (°C)	T_m (°C)	ΔH_m (J/g)
B-lignin/PLA 100/0	55.9	–	–
B-lignin/PLA 90/10	44.4	159	1.52
B-lignin/PLA 75/25	50.8	162	6.68
B-lignin/PLA 50/50	53.3	164	25.17
B-lignin/PLA 0/100	60.9	169	41.02

The phase miscibility between B-lignin and PLA was also obvious from the melting temperature of the crystalline phase in PLA. The melting temperature (T_m) and the heat of melting (ΔH_m) of the blends are listed in Table 1. Both T_m and ΔH_m decreased with an increase in B-lignin concentration in the blends. The reduction in melting temperature and enthalpy of melting was primarily caused by the reduction in chemical potential of the crystalline PLA phase as a result of molecular level miscibility with B-lignin. It also confirmed that the blends were becoming more amorphous with the increase in lignin concentration. Fibers with high PLA content were easily stabilized (a process required to gradually oxidize and stabilize lignin fibers for the subsequent carbonization process) without losing the shape of the fiber. However, fibers with high B-lignin content were preferred to ensure high carbon yield in the fibers. Therefore, a balance between PLA and lignin concentration in the precursor fibers was necessary to spool fine fibers that would maintain their structure during the thermal treatment and yield high carbon content in the carbonized fibers. Therefore, the B-lignin/PLA 75/25 blend was considered the proper precursor composition.

3.3. Influence of PLA on the thermal stability of B-lignin/PLA blends

The thermal stability of B-lignin, PLA, and their blends was investigated using thermogravimetric analysis (TGA). The TGA profiles are shown in Fig. 4. The temperatures for the onset of maximum degradation (T_{max}) taken from the peak temperature of the derivative wt.%

curves are listed in Table 2. The thermal degradation profiles and T_{max} of the investigated materials revealed a systematic enhancement in thermal stability of the blends with increasing PLA content from 0 to 50 wt.%. Pure PLA was stable without major weight loss up to 368 °C, while B-lignin and blends of PLA and B-lignin showed a continuous decrease in weight loss. The effect of blending PLA into B-lignin on the peak behavior of T_{max} was attributed to the presence of molecular level interactions between the two phases.

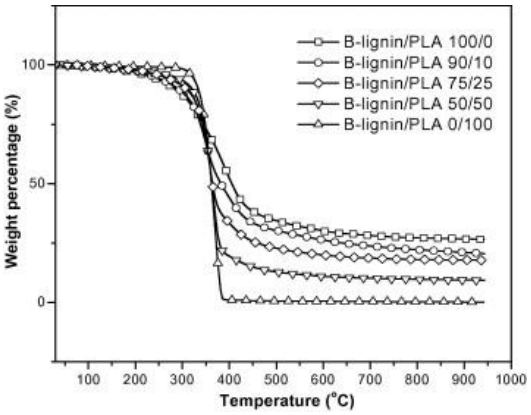

Fig. 4: Thermogravimetric analysis (TGA) weight loss curves of B-lignin/PLA blends.

Table 2: Characteristic thermal degradation temperatures (T_{max}) and wt.% of residual carbon from TGA curves.

Sample	T_{max} (°C)	Residual carbon at 800 °C (wt.%)
B-lignin/PLA 100/0	393	27.3
B-lignin/PLA 90/10	348	22.38
B-lignin/PLA 75/25	358	17.99
B-lignin/PLA 50/50	364	9.8
B-lignin/PLA 0/100	368	0.36

The rate of degradation after T_{max} was significantly higher in pure PLA than in B-lignin and their blends. As soon as temperatures surpassed T_{max}, PLA underwent depolymerization and monomer volatilization, while a gradual weight loss was observed in samples with lignin up to 400 °C, followed by a constant residual weight plateau. Hirohisa et al. [25] reported that the thermal degradation of kraft lignin occurred over a wide temperature range. The TGA curves of B-lignin and B-lignin/PLA blends (between 200 and 600 °C) were in good agreement with these reported results. In general, a major degradation step with complete decomposition of the cyclic aromatic structure of lignin in oxygen-rich atmosphere or condensation of the same structure to carbon-rich material under inert atmosphere was expected above 400 °C. In the present work, the tests were conducted under inert atmosphere so that the residual weight formed above 500 °C was primarily attributed to the condensation of cyclic structures into carbon-rich material. The residual wt.% plateau above 400 °C was stable and did not show weight loss up to 950 °C. The carbon yield measured from the residual wt.% at 800 °C decreased from 27 to 0.36 wt.% with an increase in PLA content (Table 2). Because of the complete volatilization of PLA, lignin was the main source of carbon content in the carbonized blends; therefore, optimizing the precursor

composition with a high lignin concentration will result in high carbon yields in the post carbonized fibers. Although PLA supports spinning lignin fibers, it adversely effects the carbon yields. At 50 wt.% of B-lignin in the blends, the expected carbon yield should be 13.5%, whereas the TGA results show 9.8%. The difference in the carbon yields between expected and experimental results reveals the fact that, presence of PLA in B-lignin increases the oxidation of B-lignin before conversion to carbon.

3.4. Tensile mechanical properties of raw fibers from B-lignin/PLA blends

Tensile tests were conducted with B-lignin/PLA blend fibers and pure PLA fibers. Pure B-lignin fibers were too brittle to test, therefore they were not evaluated. The stress–strain curves of pure PLA and B-lignin/PLA blends are shown in Fig. 5a and the corresponding Young's modulus and tensile strain at break measured from the stress–strain curves are shown in Fig. 5b. Significant differences in the stress–strain curves were found with increase in B-lignin concentration in the blends. Pure PLA fibers exhibited the highest tensile strength and strain at break compared to B-lignin/PLA blends. Increases in wt.% of B-lignin in the blends had detrimental effects on the mechanical properties. The high mechanical properties of pure PLA fibers are a result of the semi-crystalline nature of PLA. The crystalline phase in the polymer matrix provides rigid crosslinking sites, enhancing the stiffness of the material similar to the crosslinking density in thermoset resins [26]. In addition, the orientation of the crystalline structure may contribute to an increase in mechanical properties.

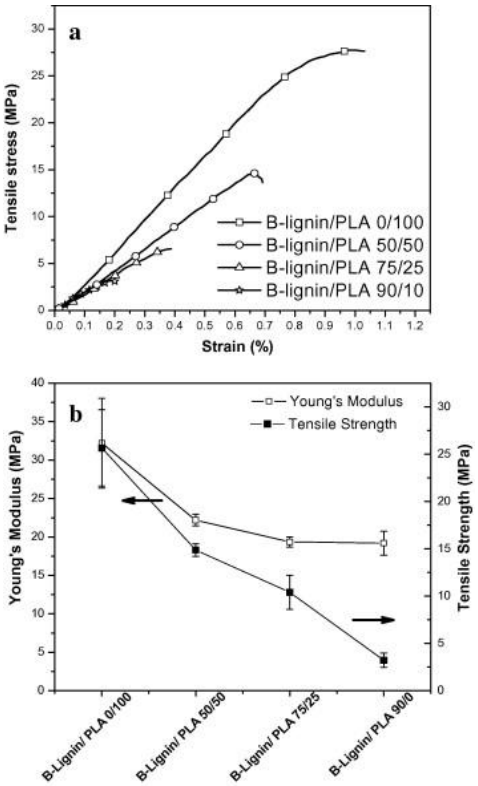

Fig. 5: Tensile mechanical properties of B-lignin/PLA precursor fibers. (a) Influences of blend composition on the stress–strain behavior of the fibers. (b) Young's modulus and tensile strain at break determined by tensile test data.

The transition in the phase morphology of the fibers seems to have significant influence on the ultimate mechanical properties. The transition in the morphologies from continuous PLA to continuous lignin phase with increase in lignin concentration resulted in showing decreasing trend in mechanical properties (modulus, strength, and strain at break) of the blend fibers. As the mechanical properties of the raw fibers significantly influenced the processability and stretchability of the fibers during the stabilization steps, B-lignin/PLA 75/25 blend fibers may be the most stable precursor fibers because of their moderate mechanical properties combined with high lignin concentration (75 wt.%).

3.5. Influence of blending with PLA on the structure of carbon fibers

The precursor fibers from pure B-lignin and B-lignin/PLA blends were converted to carbon fibers by thermostabilization at 250 °C followed by carbonization at 1000 °C. The SEM micrographs in Fig. 6 show the overall structure of the post-carbonized fibers and their cross-section morphologies. All fibers were stabilized prior to carbonization to prevent fiber fusion during the high temperature carbonization process [27]. Stabilization of raw fibers preserved the shape of the fibers during the post processing steps. During stabilization of conventional PAN-based precursor fibers, the linear polymer chains were converted to form interconnected, cyclic structures at elevated temperatures (~280 °C) that enhanced the stability of the fiber. However, lignin-based raw fibers with high lignin concentrations melted and formed ribbon-like structures, because the softening temperature (T_g) of B-lignin after butyration was ca. 50 °C. However, fibers with high PLA concentration maintained their shape because of their crystalline phase. As expected, the post-carbonized fibers with 90 and 100 wt.% of B-lignin deformed from their initially cylindrical shape to a profile with a flat surface because of melting in the fibers, while fibers with 75 and 50 wt.% of B-lignin showed cylindrical fiber structures. This further indicated that the PLA phases supported the integrity of the fiber during subsequent carbonization.

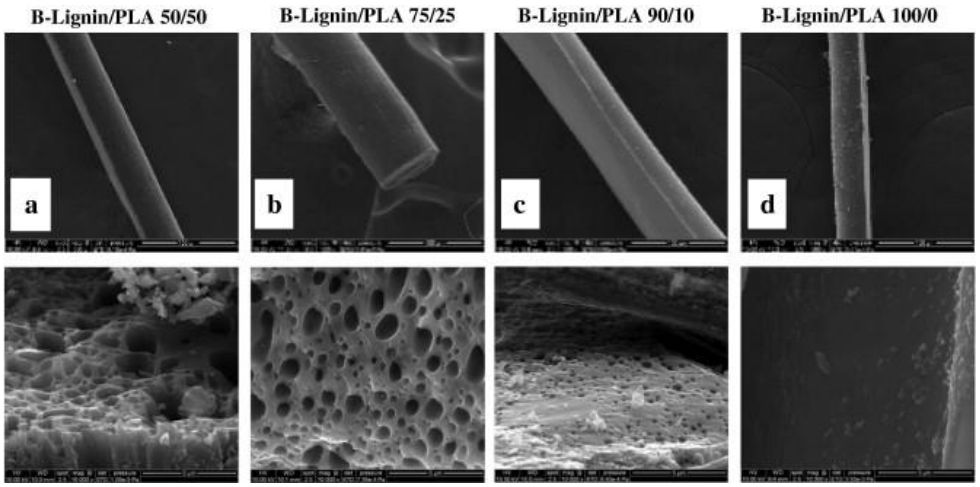

Fig. 6: SEM images of carbon fibers from B-lignin/PLA blends. Micrographs showing overall structure of the fiber (top) and cross-section images of the fibers (bottom); B-lignin/PLA (w/w): (a) 50/50; (b) 75/25; (c) 90/10; (d) 100/0.

The cross section analysis of the carbon fibers revealed the presence of microvoids in the cross section of all fibers (cross-section SEM images shown in Fig. 6), except for pure B-lignin fibers. A similar type of porous morphology was observed by Tomizuka et al. [28] and attributed to processing defects in the fibers. However, the porous morphologies in the present samples were caused by the PLA, which was blended with B-lignin to improve processability during the fiber spinning process. As the PLA depolymerized and volatilized completely above 370 °C, it produced voids in the fibers after carbonization. It can be seen that the size of the microvoids decreased with increasing B-lignin content, and the voids were not seen in the pure B-lignin carbon fibers. Compared to B-lignin/PLA 90/10 and 50/10, B-lignin/PLA 75/25 exhibited a more uniformly distributed microvoid structure. The porosity in the B-lignin/PLA carbonized fibers was quantified by Brunauer, Emmett, and Teller (BET) analysis. The porosity of the carbon fibers prepared from B-lignin/PLA 75/25 blends was compared to the commercial PAN-based carbon fibers. The BET surface area corresponding to the total surface area of the pores in the bulk fibers increased from 5.13 m^2/g in standard carbon fiber to 535 m^2/g in the B-lignin/PLA 75/25-based carbon fibers. Together with the surface area, the total volume of the pores increased from 7.68×10^{-3} cc g^{-1} to 0.323 cc g^{-1}.

4. Conclusion

Softwood kraft lignin was successfully modified following butyration reaction, and samples before and after modification were analyzed by NMR spectroscopy. B-lignin/PLA blends were prepared by melt mixing and fine fibers were successfully drawn from the blends. DSC analysis revealed the presence of single but broad T_g's for B-lignin/PLA blends, indicative of a highly compatible blend. A homogeneous, fine fiber structure was seen by SEM and the phase behavior in the B-lignin/PLA blend fibers was examined by TEM. TGA curves provided information about the influence of blending with PLA on the thermal degradation profile of lignin. Blends of B-lignin/PLA 75/25 may be the desirable composition for future carbon fiber production due to overall high compatibility, storage modulus and lignin content (therefore higher carbon yields in the carbonized fibers). The raw fibers from all the blend compositions were carbonized and cross-section analysis of the carbon fibers shows a porous microstructure in all the fibers with PLA.

Acknowledgements

The authors would like to acknowledge the support of the Iowa Alliance for Wind Innovation and Novel Development (IAWIND) and Siemens Wind Energy for funding this research work.

References

[1] S.J. Lewis. The use of carbon fiber composites on military aircraft. Compos Manuf, 5 (1994), pp. 95–103.

[2] Warren CD. ORNL Carbon fiber technology development, Oak Ridge national laboratory project report, Oak Ridge, Tennessee; 2009.

[3] J.F. Kadla, S. Kubo, R.A. Venditti, R.D. Gilbert, A.L. Compere, W. Griffith. Lignin-based carbon fibers for composite fiber applications. Carbon, 40 (15) (2002), pp. 2913–2920

[4] K. Sudo, K. Shimizu, N. Nakashima, A. Yokoyama. A new modification method of exploded lignin for the preparation of a carbon fiber precursor. J Appl Polym Sci, 48 (8) (1993), pp. 1485–1491

[5] W.L. Griffith, A.L. Compere, C.F. Leitten Jr., J.T. Shaffer. Low cost carbon fibers from renewable resources. SAMPE Int Technol Conf J, 34 (2002), pp. 959–967

[6] K. Freudenberg, A.C. Neish. Constitution and biosynthesis of lignin. Springer-Verlag (1968) p. 129–32

[7] S. Kubo, J.F. Kadla. Lignin-based carbon fibers: effect of synthetic polymer blending on fiber properties. J Polym Environ, 13 (2) (2005), pp. 97–105

[8] S. Kubo, J.F. Kadla. Kraft lignin/poly(ethylene oxide) blends: effect of lignin structure on miscibility and hydrogen bonding. J Appl Polym Sci, 98 (3) (2005), pp. 1437–1444

[9] D. Feldman, D. Banu, M. Lacasse, J. Wang, C. Luchian. Chemical modification, properties, and usage of lignin. J Macromol Sci Part A, 32 (8–9) (2002), pp. 81–99

[10] T. Miyata, T. Masuko. Crystallization behavior of poly (l-lactide). Polym J, 39 (22) (1998), pp. 5515–5521.

[11] Y. He, Z. Fan, J. Wei, S. Li. Morphology and melt crystallization of poly(l-lactide) obtained by ring opening polymerization of l-lactide with zinc catalyst. Polym Eng Sci, 46 (11) (2006), pp. 1583–1589

[12] Y. Ikeda, K. Jamshidi, H. Tsuji, S.H. Hyon. Stereocomplex formation between enantiomeric poly (lactides). Macromolecules, 20 (1987), pp. 904–906

[13] Glasser WG, Kelley SS, Rials TG, Ciemniecky SL. In: Proc. 1986 TAPPI Res. Dev. Conf.; Atlanta, Ga. Technical Association of the Pulp and Paper Industry 1986. p. 157–61.

[14] W.G. Glasser, R.K. Jain. Lignin derivatives. I. Alkanoates. Holzforschung, 47 (1993), pp. 225–233

[15] J.H. Lora, W.G. Glasser. Recent industrial applications of lignin: a sustainable alternative to nonrenewable materials. J Polym Environ, 10 (2002), pp. 39–48

[16] C.-F. Wu Leo, W.G. Glasser. Engineering plastics from lignin. I. Synthesis of hydroxypropyl lignin. J Appl Polym Sci, 29 (4) (1984), pp. 1111–1123.

[17] S.S. Kelley, W.G. Glasser, T.C. Ward. Engineering plastics from lignin. XIV. Characterization of chain-extended hydroxypropyl lignins. J Wood Chem Technol, 8 (3) (1988), pp. 341–359

[18] W. Thielemans, R.P. Wool. Lignin esters for use in unsaturated thermosets: lignin modification and solubility modeling. Biomacromolecules, 6 (2005), pp. 1895–1905

[19] H. Jankowska, A. Swiatkowski, J. Choma. Active carbon. Ellis Horwood, Chichester, UK (1991)

[20] L. Yaodong, K. Satish. Recent progress in fabrication, structure, and properties of carbon fibers. Polym Rev, 52 (3–4) (2012), pp. 234–258

[21] J. Ozaki, N. Endo, W. Ohizumi, K. Igarashi, M. Nakahara, A. Oya, *et al.* Novel preparation method for the production of mesoporous carbon fiber from a polymer blend. Carbon, 35 (1997), pp. 1031–1033

[22] L. Ji, A.J. Medford, X. Zhang. Fabrication of carbon fibers with nanoporous morphologies from electrospun polyacrylonitrile/poly(l-lactide) blends. J Polym Sci Part B: Polym Phys, 47 (5) (2009), pp. 493–503.

[23] Lue J. Lignin based carbon fibers [Ph.D. dissertation]. The University of Maine; May 2010.

[24] S. Kubo, N. Ishikawa, Y. Uraki, Y. Sano. Preparation of lignin fibers from softwood acetic acid lignin – relationship between fusibility and the chemical structure of lignin. Mokuzai Gakkaishi, 43 (8) (1997), pp. 655–662.

[25] Y. Hirohisa, M. Roland, P.K. Knut, H. Hyoe. Fractionation of kraft lignin by successive extraction with organic solvents. II. Thermal properties of kraft lignin fractions. Holzforschung, 41 (3) (1987), pp. 171–176

[26] S.L. Rosen. Fundamental principles of polymer materials. John Wiley (1993) p. 84

[27] S. Kubo, Y. Uraki, Y. Sano. Preparation of carbon fibers from softwood lignin by atmospheric acetic acid pulping. Carbon, 36 (7–8) (1998), pp. 1119–1124

[28] I. Tomizuka, T. Kurita, Y. Tanaka, O. Watanabe. Voids in the carbon fibers produced from lignin and PVA. Nippon Seram Kyo Gak, 79 (12) (1971), pp. 460–469